A non-covalent peptide-based carrier for in vivo delivery of DNA mimics

May C Morris, E. Gros, Gudrun Aldrian-Herrada, M. Choob, J. Archdeacon, F. Heitz, G. Divita

Published online 5 March 2007

Nucleic Acids Research, 2007, Vol. 35, No. 7 ***e49***
doi:10.1093/nar/gkm053

A non-covalent peptide-based carrier for *in vivo* delivery of DNA mimics

May C. Morris[1], Edwige Gros[1], Gudrun Aldrian-Herrada[1], Michael Choob[2], John Archdeacon[2], Frederic Heitz[1] and Gilles Divita[1,*]

[1]Centre de Recherches en Biochimie Macromoléculaire, Department of Molecular Biophysics and Therapeutics, FRE-2593 CNRS, 1919 Route de Mende, 34293 Montpellier, France and [2]Active Motif, Carlsbad, California, USA

Received October 4, 2006; Revised January 16, 2007; Accepted January 17, 2007

ABSTRACT

The dramatic acceleration in identification of new nucleic-acid-based therapeutic molecules has provided new perspectives in pharmaceutical research. However, their development is limited by their poor cellular uptake and inefficient trafficking. Here we describe a short amphipathic peptide, Pep-3, that combines a tryptophan/phenylalanine domain with a lysine/arginine-rich hydrophilic motif. Pep-3 forms stable nano-size complexes with peptide-nucleic acid analogues and promotes their efficient delivery into a wide variety of cell lines, including primary and suspension lines, without any associated cytotoxicity. We demonstrate that Pep-3-mediated delivery of antisense-cyclin B1-charged-PNA blocks tumour growth *in vivo* upon intratumoral and intravenous injection. Moreover, we show that PEGylation of Pep-3 significantly improves complex stability *in vivo* and consequently the efficiency of antisense cyclin B1 administered intravenously. Given the biological characteristics of these vectors, we believe that peptide-based delivery technologies hold a true promise for therapeutic applications of DNA mimics.

INTRODUCTION

The design of potent systems for the delivery of charged and non-charged molecules that target genes of interest remains a major challenge in therapeutics (1–3). Among antisense DNA mimics, peptide nucleic acids (PNAs) and their derivatives are very promising tools for antisense therapy in both eukaryotic and prokaryotic cells, as they present several advantages including specific gene targeting, high stability, resistance to nucleases and proteases, and bind RNA and DNA targets in a sequence-specific manner with high affinity (4,5). However, as for many large macromolecules, therapeutic applications of unmodified PNAs remain limited by their low cellular uptake and poor ability to reach their intracellular target (1,5,6). Recently, substantial progress has been made in the development of cell penetrating peptide-based drug delivery systems that are able to overcome both extracellular and intracellular limitations (7–9). The family of cell penetrating peptides (CPPs) includes several peptide sequences: synthetic and natural cell-permeable peptides, protein transduction domains (PTDs) and membrane-translocating sequences which have been successfully used to improve the delivery of covalently linked peptides/proteins or antisense molecules into cells (7–11). Several chemical modifications based on covalently linked cell-penetrating peptides have been successfully used to improve PNA and PNA analogue delivery into cultured cells (5,6,11–14) as well as PNA bioavailability and activity *in vivo* (5,15). As an alternative to covalent PTDs, we have designed a strategy for the delivery of different cargoes into mammalian cells, based on a short amphipathic peptide carrier that does not require prior chemical covalent coupling or denaturation steps (16–18). We have previously proposed a novel technology that combines a non-covalent peptide-based delivery system, Pep-2 (19,20) with a negatively charged PNA-like DNA mimic, HypNA-*p*PNA, (Figure 1A) consisting of a phosphonate analogue of a PNA and a PNA-like monomer based on a trans-4-hydroxyl-L-proline (21). In the present work, we describe a rational structure-based design of a new peptide carrier, Pep-3, that forms stable nano-size complexes with both uncharged and charged PNAs and promotes their cellular uptake in different cell lines. Moreover, we have elaborated a Pep-3-based protocol for systemic intravenous or intratumoral administration of a potential therapeutic antisense HyPNA-*p*PNA targeting cyclin B1 into a xenografted animal tumour model. Pep-3-mediated delivery is the first non-covalent approach described so far that allows *in vivo* delivery of DNA mimics. Our study not only demonstrates the potency of Pep-3 for delivery of

*To whom correspondence should be addressed. Tel: +33 04 67 61 33 92; Fax: +33 04 67 52 15 59; Email: gilles.divita@crbm.cnrs.fr

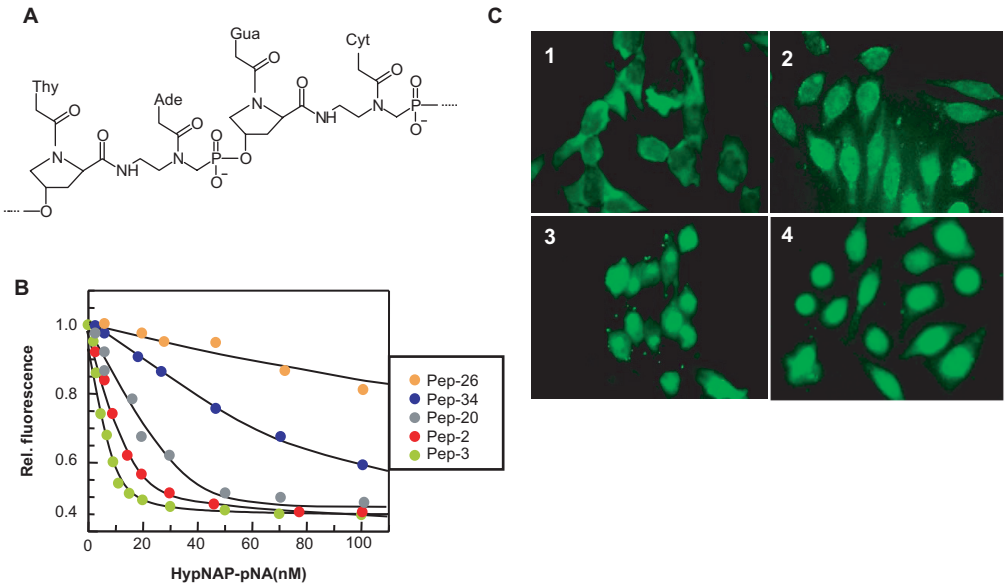

Figure 1. Evaluation of Pep-2-peptide derivatives. (**A**) Chemical structure of the DNA mimics; HypNA-*p*PNA. (**B**) Binding of peptide carrier to HypNA-*p*PNA as monitored by intrinsic fluorescence. Tryptophan fluorescence was excited at 290 nm and emission was measured at 340 nm. A fixed concentration of 100 nM of peptide Pep-3 (green), Pep-2 (red), Pep-20 (grey), Pep-34 (blue) and Pep-26 (orange), was titrated with increasing concentrations of HypNA-*p*PNA. Curves were fitted according to a quadratic equation and dissociation constants estimated to 15 ± 2 nM, 37 ± 8 nM, 104 ± 12 nM, 0.47 ± 0.12 μM and 5.2 ± 0.7 μM for Pep-3, Pep-2, Pep-20, Pep-34 and Pep-26, respectively. Results correspond to the means of four separate experiments. Pep-mediated cellular uptake of PNA and HypNA-*p*PNA. (**C**) A concentration of 0.5 μM of fluorescently labelled HypNA-*p*PNA was mixed with Pep-29 (panel 1), Pep-32 (panel 2), Pep-3 (panel 3) at a molar ratio 1/20, incubated for 30 min at 37°C, then overlaid onto cultured HeLa cells for 1 h, after which cells were extensively washed prior to observation on living cells. Similar experiments were performed with fluorescently labelled PNA mixed with Pep-3 at a molar ratio of 1:20 (panel 4).

DNA mimics into different cell lines and *in vivo* but also constitutes a major improvement over existing methods.

MATERIALS AND METHODS

Peptide synthesis and analysis

All peptides were synthesized by solid-phase peptide synthesis using AEDI-expansin resin with a 9050 Pep Synthesizer (Millipore, Wartford, UK) according to Fmoc/tBoc method and purified as already described (16,17) on a pioneer peptide synthesizer (Pioneer™, Applied Biosystems, Foster City, CA, USA) starting from Fmoc-PAL-PEG-PS resin at a 0.2 mmol scale. The coupling reactions were performed with 0.5 M of HATU in the presence of 1 M of DIEA. Protecting group removal and final cleavage from the resin were carried out with TFA/Phenol/H_2O/Thioanisol/Ethanedithiol (82.5/5/5/5/2.5%) for 3 h 30 min. All peptides were N-acetylated and bear a cysteamide group at their carboxy-terminus (-NH-CH_2-CH_2-SH). The crude peptide was purified by RP-HPLC on a C^{18} column (Interchrom UP5 WOD/25M Uptispere 300 5 ODB, 250×21.2 mm). Electrospray ionization mass spectra were in complete agreement with the proposed structure. Mono-PEGylated-Pep-3 conjugation was performed at the primary amino group of the N-terminal residues, using aldehyde monoethoxypoly(ethylene glycol) at pH 5.5, then PEGylated-peptide was further purified by RP-HPLC and analysed by electro spray ionization mass spectroscopy (16,17).

PNA and HypNA-*p*PNA synthesis

Classical PNAs were obtained from Applied Biosystems (Foster city, CA, USA) and HypNA-*p*PNAs were made by solid-phase synthesis using a derivatized CPG support on a DNA synthesizer (Applied Biosystems 380B automated DNA synthesizer) as previously described and obtained by Active Motif Inc. (21) sequences correspond to the 18 mer antisense PNA. Three different antisense sequences were used, targeting respectively the first codons, Cyc-B1a (TGC CAT CGG GCT TGG AGG) and Cyc-B1c (GCG CTT TGC GCC TGC CAT) and position 475–492, Cyc-B1b (TCC ATC TTC TGC ATC CAC) of the open reading frame the cyclin B1 gene. A sequence derived from Cyc-B1a harbouring two mismatches, Cyc-$B1^{mm}$ (TGC CAT CAG GCT TAG AGG) and an antisense sequence targeting firefly luciferase (TGG CGT CGG TGA CCA TT) were used as controls to validate target specificity.

Proteins and antibodies

Mouse monoclonal anti-cyclin B1 antibodies (SC-245) and rabbit polyclonal anti-cdk2 antibodies (SC-163) for western blotting were obtained from Santa Cruz Biotechnology Inc. (Santa Cruz, CA, USA).

Cell culture and Pep-mediated transfection

Adherent fibroblastic HeLa, primary human umbilical vein endothelial cells (HUVEC), Jurkat T, PC3 and MCF-7 cell lines (from American Type culture collections; ATCC) were cultured in Dulbecco's Modified Eagle's Medium supplemented with 2 mM glutamine, 1% antibiotics (streptomycin 10 000 µg/ml, penicillin, 10 000 IU/ml) and 10% (w/v) foetal calf serum (FCS), at 37°C in a humidified atmosphere containing 5% CO_2. For Peptide- (Pep-2, Pep-3, MPG) mediated delivery of PNA and HypNA-*p*PNA, stock solutions of HypNA-pPNA/peptide and PNA/peptide complexes were formed by incubation of antisense HypNA-*p*PNA or PNA with carrier peptide at a molecular ratio of 1/20 in PBS for 30 min at 37°C, then were diluted to the required concentration in 500 µl of DMEM. Cells grown to 60% confluence were then rinsed twice and overlaid with preformed complexes. After a 30-min incubation at 37°C, 1 ml of fresh DMEM supplemented with 10% foetal calf serum was added directly to the cells, without removing the overlay of PNA/peptide or HypNA-*p*PNA/peptide complexes, and cells were returned to the incubator for 24 h. For suspension cell lines, cells were harvested by centrifugation and resuspended directly with the preformed complex solutions for 5 min and then the level of foetal calf serum was adjusted to 10%. Lipid-based delivery of HypNA-*p*PNA, transfections were performed with Lipofectamine 2000 (Invitrogen, Carlsbad, CA, USA), according to the protocols used for Pep-3 and described in the manufacturer's guidelines. Cyclin B1 protein levels were determined after 24 h by western blotting. For cellular localization experiments, cells were grown on acid-treated glass coverslips to 60% confluence and then overlaid with preformed antisense/peptide complexes. After 1 h, cells were rinsed twice and cellular localization of FITC-labeled HyPNA-*p*PNA and PNA was monitored by fluorescence microscopy on living cells.

Cytotoxicity assay

The cytotoxicity side effects of the different HypNA-*p*PNA/carrier complexes were determined with a MTT assay after 24 h. HUVEC and Jurkat T cell lines were cultured for 24 h prior incubation with different HypNA-*p*PNA/carrier preparations. In order to evaluate the toxicity associated to antisense/carrier complexes, the different carriers were associated to the control mismatch antisense Cyc-B1^{mm} HypNA-*p*PNA sequence. The specific antisense response was then calculated as a ratio of cyclin B1 to total protein and corrected for toxicity of the complexes.

Mouse tumour model

Athymic female nude mice (6–8 weeks of age) were subcutaneously inoculated in the flank with 1×10^6 PC3 cells in 100 µl PBS. A week after tumour implant, when tumour size reached ~50–100 mm^3, animals were treated by intratumoral or intravenous injection, every three days, with a solution of 0.1 or 0.2 ml of different antisense HypNA-*p*PNA formulations. Mice received either free HypNA-*p*PNA (50 or 100 µg) or HypNA-*p*PNA complexed (1, 5 and 10 µg) to Pep-3 or Pep-2 at a 20/1 molar ratio. Formulations containing 20% of PEGylated-Pep-3 were obtained by forming a precomplex HypNA-*p*PNA/Pep-3 at molar ratio of 1/5 and then increasing the ratio of antisense/carrier up to 1/20 with PEG-Pep-3. The tumour diameter was measured in two directions at regular intervals using a digital calliper and volumes were calculated using the formula length × width × height × 0.52 (22). Curves show the mean value of tumour size in a group of five animals and no animal death nor any sign of toxicity were observed. After 25 days, tumours were removed, and cyclin B1 protein levels were evaluated by western blotting. Experiments were performed according to national regulations and approved by the local animal experimentation ethical committee.

Characterization of complex formation

Fluorescence titration experiments were performed as previously described (16,23), on a PTI QuantaMaster spectrofluorometer at 25°C, using band-passes of 6 and 8 nm for excitation and emission, respectively. Tryptophan fluorescence emission was recorded over a range of 305–400 nm, with an excitation wavelength of 295 nm. A fixed concentration of carrier-peptide (100 nM) was titrated with increasing concentrations of PNA and HypNA-pPNA (between 0 and 500 nM) at 25°C in water. Fitting of titration curves was accomplished using a quadratic equation and Grafit Software (Erithacus Software Ltd) as previously described (16,23). All results correspond to the average of four separate experiments with a standard deviation smaller than 10%. Mean particle size distribution was determined with a Coulter N4 Plus (Coulter-Beckman) at 25°C for 3 min per measurement.

RESULTS AND DISCUSSIONS

Design and evaluation of peptide carriers

The sequence of Pep-2 (K E T W F E T W F T E W S Q P K K K R K V-Cya) previously described (19), was used as a template for screening new peptide vectors for *in vitro* and *in vivo* delivery of PNAs and analogues. A series of mutations and deletions were performed in order to identify the essential residues required to form stable complexes with PNAs and analogues and to improve their delivery into cells (Table 1). The impact of each residue on Pep-2 efficacy was evaluated by alanine scanning throughout the sequence of Pep-2. Moreover, as aromatic residues are required for both binding of the carrier to PNAs and cellular uptake, the impact of the position of the Trp and Phe residues in the N-terminal hydrophobic sequence was investigated. As we have previously reported that the cysteamide group at the C-terminus of peptide is required for its cellular uptake and delivery efficacy, all peptides were synthesized with a cysteamide at their C-terminus and acetylated at their N-terminus (17,18).

Table 1. Evaluation of Pep-2-peptide derivatives

Peptides	Sequences	Binding[a]	Uptake[b]
Pep-2	K E T W F E T W F T E W S Q P K K K R K V-Cya	+++	+++
Pep-20	A E T W F E T W F T E W S Q P K K K R K V-Cya	+++	−
Pep-21	K A T W F E T W F T E W S Q P K K K R K V-Cya	+++	+++
Pep-22	K E A W F E T W F T E W S Q P K K K R K V-Cya	++	++
Pep-23	K E T A F E T W F T E W S Q P K K K R K V-Cya	−	−
Pep-24	K E T W A E T W F T E W S Q P K K K R K V-Cya	−	−
Pep-25	K E T W F A T W F T E W S Q P K K K R K V-Cya	++	++
Pep-26	K E T W F E A W F T E W S Q P K K K R K V-Cya	+	−
Pep-27	K E T W F E T A F T E W S Q P K K K R K V-Cya	−	−
Pep-28	K E T W F E T W A T E W S Q P K K K R K V-Cya	−	−
Pep-29	K E T W F E T W F A E W S Q P K K K R K V-Cya	+++	+++
Pep-30	K E T W F E T W F T A W S Q P K K K R K V-Cya	+++	+++
Pep-31	K E T W F E T W F T E A S Q P K K K R K V-Cya	+++	++
Pep-32	K E T W F E T W F T E W A Q P K K K R K V-Cya	+++	+++
Pep-33	K E T W F E T W F T E W S A P K K K R K V-Cya	+++	+++
Pep-34	K E T W F E T W F T E W S Q A K K K R K V-Cya	++	−
Pep-35	K E T W F E T W F T E W S Q P A K K R K V-Cya	+++	+
Pep-36	K E T W F E T W F T E W S Q P K A K R K V-Cya	+++	+
Pep-37	K E T W F E T W F T E W S Q P K K A R K V-Cya	+++	++
Pep-38	K E T W F E T W F T E W S Q P K K K A K V-Cya	+++	+
Pep-39	K E T W F E T W F T E W S Q P K K K R A V-Cya	+++	+
Pep-40	K E T W F E T W F T E W S Q P K K K R K A-Cya	+++	+++
Pep-41	W F K E T E T W F T E W S Q P K K K R K V-Cya	++	−
Pep-42	K W F E T E T W F T E W S Q P K K K R K V-Cya	+++	++
Pep-42	K E W F T E T W F T E W S Q P K K K R K V-Cya	+++	++
Pep-43	K E T W F E T W F T E W S Q P K K K R K V-Cya	+++	+++
Pep-44	K E T E W F T W F T E W S Q P K K K R K V-Cya	++	−
Pep-45	K E T E T W F W F T E W S Q P K K K R K V-Cya	+++	−
Pep-46	K E T E T T W F W F E W S Q P K K K R K V-Cya	++	+
Pep-47	K E T E T T E W F W F W S Q P K K K R K V-Cya	+	−

[a]Binding of peptide to PNA or HypNA-*p*PNA was monitored by fluorescence spectroscopy, using the intrinsic fluorescence of the Trp residues. Data were fitted as reported in Figure 1A and symbols +++, ++, + and − correspond to dissociation constant values respectively lower than 100 nM, 500 nM, 1 μM and higher than 1 μM.

[b]Cellular uptake was determined using fluorescently labelled PNA or HypNA-*p*PNA, as described in Figure 1B, symbols +++, ++, + and − correspond to >80%, 50%, <10% and a lack of delivery efficiency, respectively.

Peptides were selected based on their ability to both form stable complexes with PNAs and HyPNA-pPNAs, and improve the cellular uptake of fluorescently labelled HyPNA-*p*PNAs. The binding to PNAs or PNA analogues was monitored by fluorescence spectroscopy, using the intrinsic fluorescence of the Trp residues located in the hydrophobic domain of the peptide as a sensor of the interaction (Figure 1B). The potency of the peptides to deliver fluorescently labelled HyPNA-*p*PNAs into cultured cells was monitored by fluorescence microscopy on living cells (Figure 1C). Typical experiments and data are reported in Figure 1. Our results reveal that major interactions between DNA mimics and the peptide carrier are mediated by the hydrophobic domain of the peptide and that tight binding of the carrier to PNA analogues, with nanomolar affinity, is a prerequisite for efficient delivery. However, results obtained with peptides Pep-20 and Pep-34 to Pep-39 (Table 1) indicate that this feature alone is insufficient and that the number of charges also plays a critical role for efficient cellular uptake. These results enabled us to identify key residues required for optimal carrier functions and to propose the following rules for sequence optimization. Irrespective of the sequence of the hydrophobic moiety of the peptide, a minimum of four cationic residues is required within the hydrophilic domain. The number of charged residues has a major impact on the initial electrostatic interactions of the peptide with the cell membrane components as already reported for several cell-penetrating peptides (24–26). In addition, three residues are critical for both delivery and solubility of the peptide, the charged N-terminal Lys^1 residue, Thr^7 between the two Trp-Phe motifs and Pro^{14} in the linker motif that enables flexibility between the hydrophobic and the hydrophilic domains. The position of the Trp-Phe tandem in the hydrophobic sequence is equally critical for cell entry of the peptide carrier associated with PNAs or PNA analogues. Structural characterization of Pep-1 and Pep-2 has shown that the N-terminal hydrophobic sequence of the peptide has the tendency to adopt an alpha helical structure at high concentration or in the presence of lipids (23). Projection of the helical domain in Pep-2 reveals that all aromatic residues create an interaction patch located on the same side of the helix (Figure 2B). Based on our peptide screen, it is clear that this helical organization should be taken into account for optimization of peptide carriers, and any modifications that even slightly affect binding to cargoes may have a dramatic impact on cellular uptake. These results strengthen the notion that the helical organization of Pep carriers is a determining factor for their interaction with the cell membrane, thereby enabling aromatic residues on this helix to interact with lipids and

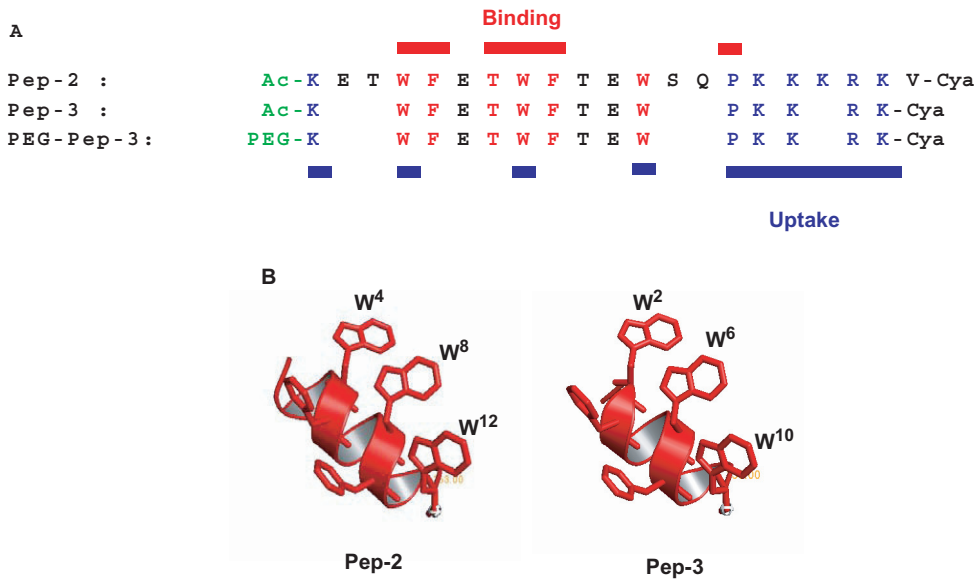

Figure 2. Sequence alignment and structural properties of Pep-2 and Pep-3. (**A**) sequence alignment of the different peptide carriers. Residues involved in cargo binding and cellular uptake are in red and blue, respectively. Structural model of Pep-2 and Pep-3. The structure of Pep-3 was elaborated based on the structure of Pep-1, previously determined by NMR[23], using Discover/Insight II package (MSI Inc., San Diego, USA) and Delano Scientific LLC Pymol software (San Carlo, USA).

consequently favouring membrane disorganization, as previously suggested (23).

Taking these rules into account, we designed a 15-residue peptide; Pep-3 (ac-K W F E T W F T E W P K K R K-Cya), that bears all residues required for efficient uptake of HyPNA-*p*PNAs and has a tendency to adopt a helical structure within membranes. Pep-3 interacts with PNAs and PNA analogues with a dissociation constant of ~10–20 nM depending on the nature of the cargo (Figure 1B). Saturation of Pep3/HyPNA-*p*PNA complex formation occurs for a molar peptide/cargo ratio of ~20, which is in perfect agreement with our previous finding for Pep-1 and derived peptides (17,23). As reported in Figure 1C (panel 3 and 4), Pep-3 significantly facilitates cellular uptake of both PNAs and HypNA-*p*PNAs. Determination of the size of these particles by light scattering reveals that Pep-3 forms stable particles with HyPNA-*p*PNAs ($K_d = 15 \pm 2$ nM) in the range of 0.092 ± 0.01 µm diameter, in contrast to Pep-2 which exhibits a slightly lower affinity for PNAs ($K_d = 37 \pm 8$ nM) and forms average size particles of 0.34 ± 0.1 µm diameter within a more dispersed population.

Pep-3 mediated delivery of antisense HypNA-*p*PNA *in vitro*

The potency of Pep-3 to deliver HypNA-*p*PNA in a biologically relevant system was investigated using antisense targeting cyclin B1. Cyclin B1 is a non-redundant cyclin, and an essential component of 'Mitosis Promoting Factor', which it forms together with its partner protein kinase Cdk1 (27). Alteration in both expression and activation of cyclin B1 have been shown to be associated to numerous cancers, thus an antisense approach controlling cyclin B1 levels has been proposed as an anti-proliferative strategy of choice (28,29). We have designed three different antisense sequences against the open ready frame of the cyclin B1 gene: Cyc-B1a, Cyc-B1b and Cyc-B1c (Figure 3A). These antisense HypNA-*p*PNA were complexed with Pep-3 at a molar ratio of 1/20, and their impact on cyclin B1 protein levels was evaluated on Hela cells. As reported in Figure 3B, a concentration of 50 nM of antisense Cyc-B1a or Cyc-B1b HypNA-*p*PNA altered cyclin B1 protein levels by 85 and 63%, respectively, in a specific fashion by comparison to the antisense luciferase control that has no effect on cyclin B1 levels. In contrast, antisense Cyc-B1c HypNA-*p*PNA yielded a limited biological response (less than 10%), which may be due to the poor accessibility of the target sequence. Dose response analysis of the three antisense revealed that, when complexed to Pep-3, antisense Cyc-B1a and Cyc-B1b efficiently downregulate cyclin B1 protein levels in HeLa cells with an IC50 of 12 ± 3 and of 31 ± 5 nM, respectively (Figure 3B and C). However, only Cyc-B1a is able to reduce cyclin B1 levels by more than 90%. In contrast, no effect on cyclin B1 protein levels was observed in the presence of a control HypNA-*p*PNA sequence harbouring two mutations complexed with Pep-3. Given its high efficiency, antisense Cyc-B1a HypNA-*p*PNA was used throughout the rest of the study.

Pep-3 mediated delivery of antisense HypNA-*p*PNA into primary and suspension cell lines

Numerous delivery methods have been described as highly potent on commonly used adherent cell lines; in contrast, only few are able to efficiently transfect primary and suspension cell lines. In particular, toxicity is a major issue when considering the development of delivery systems for primary and suspension cell lines. Hence, prior to characterizing the specificity of antisense effect, we first evaluated the toxicity of different delivery systems

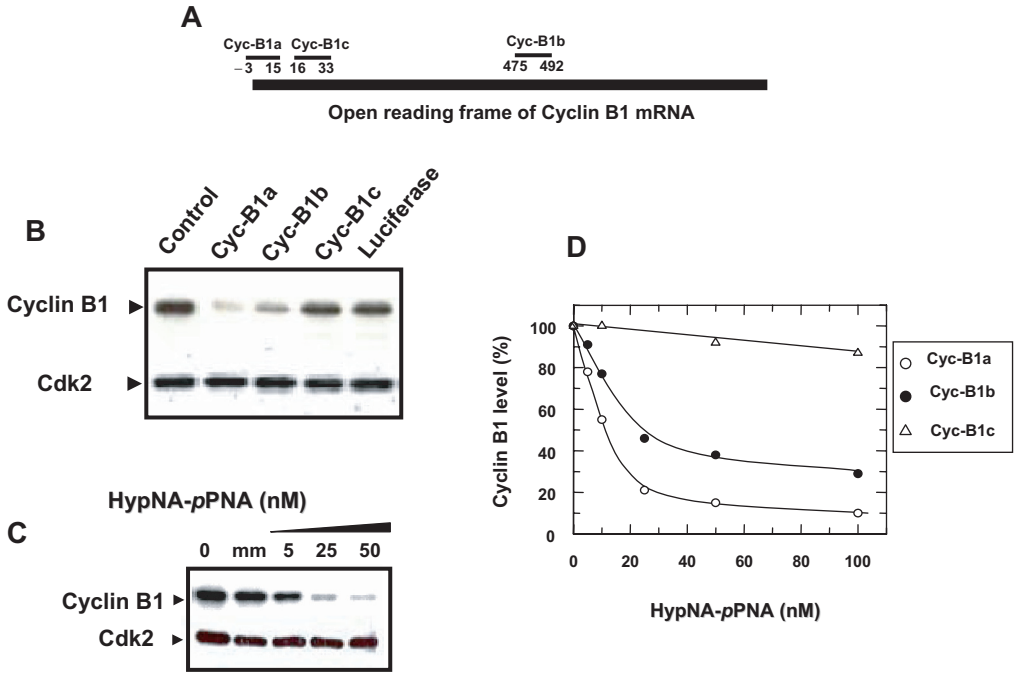

Figure 3. Pep-3-mediated delivery of an antisense cyclin B1 HypNA-*p*PNA into mammalian cells. (**A**) Hybridization sites of the three HypNA-pPNA antisenses B1 on the cyclin B1 mRNA. (**B**) A fixed concentration of 50 nM of the Cyc-B1a, Cyc-B1b, Cyc-B1c antisense HypNA-*p*PNA and luciferase antisense were incubated with Pep-3 at a molar ratio 1:20 at 37°C for one hour, then overlaid onto cultured cells. Cyclin B1 protein levels were analysed by western blotting after 30 h. Cdk2 protein was used as a control to normalize protein levels. The level of endogenous cyclin B1 in untreated cells is reported in lane control. (**C**) Increasing concentrations (5, 25, and 50 nM) of HypNA-*p*PNA Cyc-B1a were incubated with Pep-3 at a molar ratio 1:20 at 37°C for one hour, then overlaid onto cultured cells. Cyclin B1 protein levels were analysed by western blotting after 30 h. Control experiments performed with 2 μM of CycB1^{mm} (mm) HypNA-*p*PNA containing two mutations. (**D**) Dose response analysis of increasing concentrations (5, 10, 25, 50 and 100 nM) of HypNA-*p*PNA Cyc-B1a, Cyc-B1b and Cyc-B1c. HypNA-*p*PNAs were incubated with Pep-3 at a molar ratio 1:20 at 37°C for one hour, then overlaid onto cultured cells. Cyclin B1 protein levels were analysed by western blotting after 30 h.

including Pep-3, Pep-2, MPG and Lipofectamine complexed with the mismatch antisense CycB1^{mm} HypNA-pPNA on HUVEC and Jurkat T cells. On both cell lines, no significant toxicity (less than 10%), was observed with Pep-3 and Pep-2, up to a 2 μM concentration of antisense. In contrast, cell viability was reduced by ~52% (HUVEC) and 70% (Jurkat T) in the presence of Lipofectamine using the same antisense concentration. Subsequently, the efficiency of cyc-B1a HypNA-*p*PNA/Pep-3 was evaluated on different cell lines, including HUVEC, Jurkat T, MCF 7 and PC3 cell lines. Typical western blot analysis demonstrated that irrespective of the cell line, a 100 nM concentration of antisense HypNA-*p*PNA complexed with Pep-3, was sufficient for robust silencing of cyclin B1 at the protein level, ranging from 70% for Jurkat cells to 95% for HUVEC cells (Figure 4A). The potential of Pep-3 to deliver Cyc-B1a HypNA-*p*PNA into cell lines which are quite challenging to transfect, such as primary HUVECs and Jurkat was then investigated in comparison with other delivery methods including the cell penetrating peptides (Pep-2, MPG) or a cationic lipid formulation (Lipofectamine). As reported in Figure 4B, the four delivery methods used enabled delivery of cyc-B1a HypNA-*p*PNA into HUVEC cells, however the specific antisense response obtained with Pep-3 (IC_{50} of 7.2 ± 2 nM) was respectively 3-, 15- and 70-fold, greater than that obtained with Pep-2 (IC_{50}: 21 ± 5 nM), Lipofectamine (IC_{50}: 120 ± 10 nM) and MPG ($IC_{50} > 500$ nM). Remarkably, Pep-3-mediated delivery was the only strategy providing a significant and specific antisense response on Jurkat T cells, with 70–80% downregulation of cyclin B1 (IC_{50}: 24 ± 5 nM). In contrast, no significant biological response was obtained with either MPG or Lipofectamine and only a moderate antisense response was obtained with Pep-2 ($IC50 > 1.5$ μM). The relatively low efficiency of MPG on both cell lines is probably associated to the low stability of the complex. Indeed MPG has been shown to be more appropriate for delivery of nucleic acids and its hydrophobic domain does not harbour any Trp residues, which are essential to stabilize the interaction with PNA or HypNA-*p*PNA (16,18). Taken together, these results demonstrate that sequence optimization of Pep-2 to Pep-3 constitutes a major improvement over Pep-2 carrier whose efficiency is limited in suspension cell lines.

Pep-3 mediated delivery of antisense HypNA-*p*PNA targeting cyclin B1 *in vivo*

In vivo, bioavailability of DNA mimics constitutes one of the major limitations in therapeutics (1–4). The potential

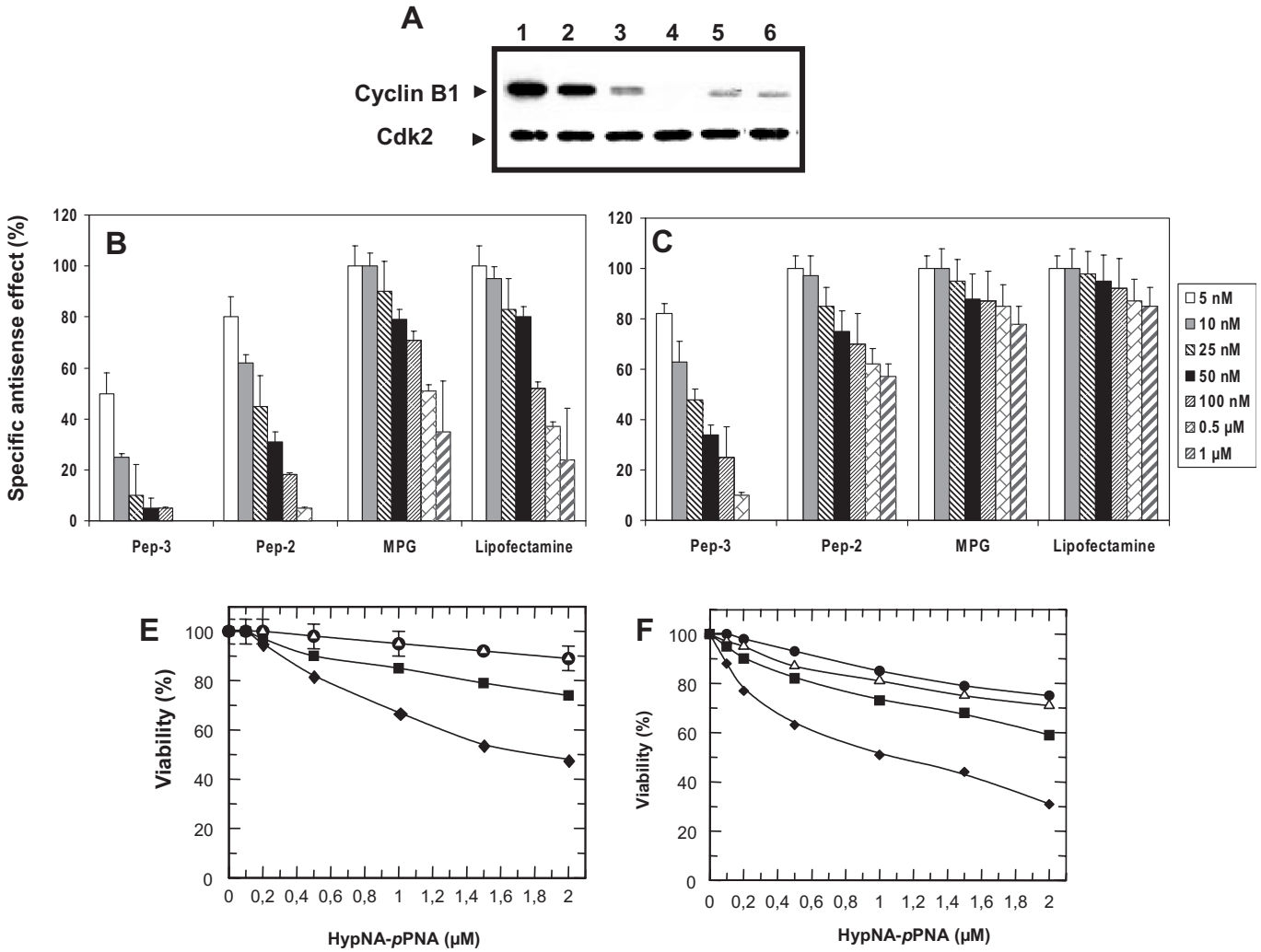

Figure 4. Pep-3-mediated delivery of an antisense cyclin B1 HypNA-*p*PNA in primary and suspension cell lines. (**A**) Pep-3-mediated delivery of antisense cyclin B1 HypNA-*p*PNA was evaluated on different cell lines. Here, 100 nM of antisense HypNA-*p*PNA was complexed with Pep-3 at a molar ratio 1:20, then evaluated on Jurkat T (lane 3), HUVEC (lane 4), PC3 (lane 5) and MCF7 (lane 6). Also, 100 nM of antisense HypNA-*p*PNA was complexed with Pep-2 at the same ratio and evaluated on Jurkat T (lane 2). The level of endogenous cyclin B1 in untreated cells is reported in lane 1. (**B/C**) Comparison of Pep-3 strategy to other delivery methods. Increasing concentrations from 5 nM to 1 µM of HypNA-*p*PNA Cyc-B1a were associated with Pep-3, Pep-2 or MPG at a molar ratio 1:20 or with Lipofectamine, then overlaid onto cultured HUVEC (panel B) and Jurkat (panel C) cells. Cyclin B1 protein levels were analysed by western blotting after 30 h and antisense effect was normalized. (**D/E**): Toxicity of the different delivery methods: HUVEC (panel E) and Jurkat (panel F) cells, were incubated with increasing concentrations of Cyc-B1^{mm} HypNA-*p*PNA complexed with Pep-3, Pep-2, MPG and Lipofectamine. Cell viability was evaluated by MTT assay after 24 h.

of Pep-3 to deliver antisense cyclin B1 HypNA-*p*PNA *in vivo* was evaluated on human prostate carcinoma cell (PC3) xenografted mice. This mouse tumour model was used to test systemic administration of Pep-3/antisense on the growth inhibition of established subcutaneous tumours. Formulations of Pep-3/HypNA-*p*PNA complexes at a 20/1 molar ratio (Figure 5A), were administered intravenously or directly into the tumour every three days, and changes in tumour size were monitored over a course of two weeks following injection. As a control, we show that administration of 50 µg (intratumorally) and 100 µg (intravenously) of naked HyPNA-*p*PNA or of Pep-3 do not produce any significant effect on tumour growth. As reported in Figure 5B, intratumoral injection of Pep-3/HyPNA-*p*PNA potently inhibits tumour growth in a concentration-dependent manner, with 50% inhibition for 1 µg and more than 92% for 5 µg of antisense HyPNA-*p*PNA. In contrast, intravenous administration of Pep-3/HyPNA-*p*PNA (10 µg of antisense) only reduces tumour growth by ~20%, whilst of Pep-2/HyPNA-*p*PNA complexes have no effect on tumour growth, supporting the idea that *in vivo* efficiency is directly associated with the size and stability of Pep-based 'nanoparticles'.

PEGylation improves Pep-3 efficiency *in vivo*

PEGylation plays a key role in drug delivery and has been reported to enhance *in vivo* potency and stability of numerous therapeutic molecules (30). As such to improve the stability of Pep-3/HypNA-*p*PNA particles *in vivo*, the sequence of Pep-3 was modified by the attachment of a

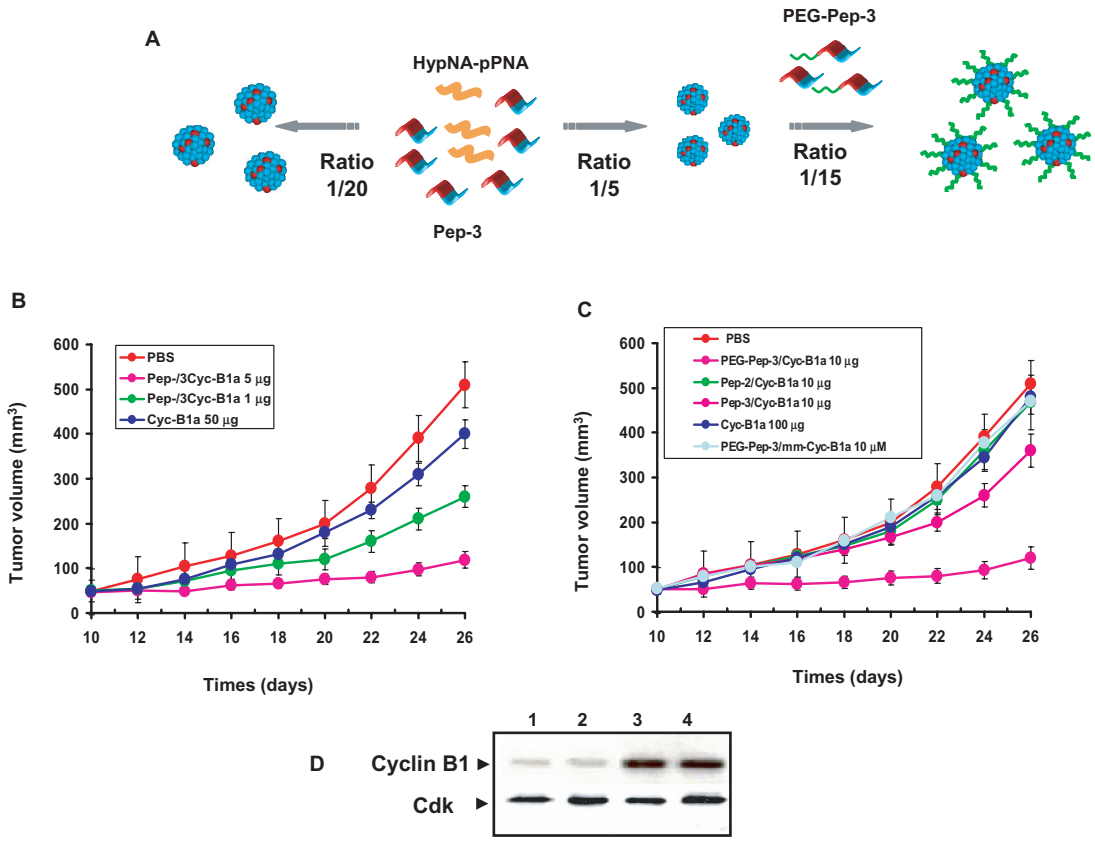

Figure 5. Pep-3-mediated delivery of an antisense cyclin B1 HypNA-*p*PNA *in vivo*. (**A**) Protocol of Pep-3/HypNA-pPNA complex formation. For intratumoral injection Pep-3/HypNA-pPNA were directly formed at a 20/1 molar ratio. Formulations containing 20% of PEGylated-Pep-3 were obtained by forming a precomplex HypNA-*p*PNA/Pep-3 at molar ratio of 1/5 and then increasing the ratio of carrier up to 1/20 with PEG-Pep-3. Formulations were incubated for 30 min at 25°C before dilution in PBS and injection. (**B**) Tumour growth inhibition by antisense HypNA/Pep-3 via intratumoral administration. Mice inoculated with PC3 tumour cells were left untreated (red circles) or treated every three days by intratumoral injection of 50 µg of naked HypNA-*p*PNA, (blue circles) or 1 (green circles) and 5 µg (fuchsia circles) of antisense associated with Pep-3. (**C**) Tumour growth inhibition by antisense HypNA-pPNA/Pep-3 via intravenous administration. Xenografted mice were treated with 100 µg of naked HypNA-pPNA (blue circle), 10 µg of antisense HyPNA-*p*PNA containing two mutations associated with PEG-Pep-3 (grey circles) or 10 µg of antisense associated with Pep-3 (orange circles), Pep-2 (green circles) and PEG-Pep-3 (fuchsia circles) at a 20:1 molar ratio. Treatment started after seven days, when tumour size reached ~50–100 mm^3. The tumour diameter was measured in two directions at regular intervals using a digital calliper. Curves represent the mean value of tumour size in a group of five animals. (**D**) Tumour cyclin B1 protein levels analysed by western blotting after 25 days. Intratumoral administration of 5 µg of antisense HypNA-*p*PNA/Pep-3 (lane 1), intravenous administration of 10 µg of antisense HypNA-*p*PNA/Pep-3/PEG-Pep-3 (lane 2) and injection of 50 µg naked HypNA-*p*PNA intratumorally (lane 3) or intravenously (lane 4). Cdk2 protein was used as a control to normalize protein levels.

polyethylene glycol (PEG) moiety at its N-terminus. We have established a protocol to obtain formulations containing PEGylated-Pep-3, in which the HyPNA-*p*PNA is first associated to unPEGylated Pep-3 at a molar ratio of 1/5, which is then adjusted to 1/20 using different concentrations of PEG-Pep-3 (Figure 5A). We found that formulations containing up to 15% of PEGylated-Pep-3 exhibit the same efficiency and ability to reduce levels of cyclin B1 on cultured cells. Xenografted mice were intravenously treated with 10 µg of antisense HypNA-*p*PNA complexed with Pep-3/PEG-Pep-3 (80/20). As shown in Figure 5C, the PEGylated formulation significantly improves delivery and stability of the complex, and efficiently inhibits tumour growth by more than 90%, which is 4–5-fold more efficient than unPEGylated Pep-3. Moreover, we demonstrated that the effect on tumour growth is sequence specific as an antisense HyPNA-*p*PNA bearing two mutations complexed to PEG-Pep-3 was unable to inhibit tumour growth. As reported in Figure 5D, the effect on tumour growth can be correlated to a decrease in the levels of cyclin B1 protein by ~60% in animals treated with Pep-3/HyPNA-pPNA (5 µg/intratumorally) or with HypNA-pPNA/Pep-3/PEG-Pep-3 (10 µg/intravenously), which is consistent with the *in vitro* antisense impact and suggests a specific effect associated with the cyclin B1 antisense.

CONCLUSIONS

Improved design and chemistry of charged and uncharged DNA mimics has yielded highly stable molecules, which exhibit high affinity for their target and low toxicity due to their efficiency (1–5). However, the challenge to their *in vivo* administration remains in their therapeutic

application, the use of low doses of DNA mimics being inapplicable *in vivo*, given their poor cellular uptake and their lack of rational targeting (3–6). In the present study, we have elaborated a strategy combining a non-covalent peptide-based delivery system and a charged PNA-like DNA mimic that is likely to have potent implications in therapeutics. HypNA-*p*PNA DNA mimics have already been used successfully both *in vitro* and *in vivo* (19,20,31,32) and offer several advantages due to their tight interaction with target DNA as well as their high solubility (21,32). Cell-penetrating peptides are most promising tools for delivery of therapeutic molecules (8,9) and the recent reconsideration of their cellular uptake mechanism has provided new perspectives for their *in vivo* application (25,26). Here, we demonstrate that key parameters need to be taken into account in the design of a non covalent peptide-based delivery strategy, including the secondary structure of the carrier, the presence of a critical number of charged and aromatic residues, as well as the size and the stability of the carrier/cargo particles. Using a rational approach we have designed a new peptide, Pep-3, which forms 'nanoparticles' with charged and uncharged PNAs and improves their delivery into a large panel of cell lines as well as into an animal model. These results reveal a correlation between biological efficiency, carrier/cargo affinity, complex stability, particle size and homogeneity. Pep-3/antisense HypNA-*p*PNA particles targeting the cell cycle regulatory protein cyclin B1 were successfully applied *in vivo* through intratumoral and intravenous administration and were found to inhibit tumour growth as efficiently as proven siRNA molecules. *In vivo* delivery of HypNA-*p*PNA is a potent strategy for several therapies. Here we demonstrate not only that a peptide-based nanoparticle system efficiently delivers such PNA mimics into living cells and animal tumour models, but also that it can be improved by PEGylation of the carrier, which stabilizes the complexes. This study shows that such a modification significantly improves Pep-3 for *in vivo* systemic administration, allowing us to reduce the dose required to induce a specific and robust biological response, thereby limiting non-specific cytotoxic effects described upon treatment with high concentrations of PNAs. Together, these data reveal that Pep-3 constitutes an excellent candidate for *in vivo* delivery of charged PNA and DNA mimics. Moreover, Pep-3 is a potent delivery approach, which is far more appropriate for suspension and primary cell lines than other currently used methods, and which exhibits far less toxicity than other delivery systems.

ACKNOWLEDGEMENTS

This work was supported in part by the Centre National de la Recherche Scientifique (CNRS) and by grants from the Agence Nationale de Recherche sur le SIDA (ANRS) and the EU (Grant QLK2-CT-2001-01451 and Grant LSHB-CT-2003-503480/TRIoH) and the Association pour la Recherche sur le Cancer to MCM (ARC-4326) and to GD (ARC-5271). We thank J. Mery for expertise on peptide synthesis. The Pep-1/Chariot project was supported by a grant from Active Motif (Carlsbad, CA, USA). Funding to pay the Open Access publication charge was provided by by the CNRS.

Conflict of interest statement. None declared.

REFERENCES

1. Opalinska,J.B. and Gewirtz,A.M. (2002) Nucleic-acid therapeutics: basis principles and recent application. *Nat. Rev. Drug Discov.*, **1**, 503–514.
2. Kurreck,J. (2003) Antisense technologies: improvement through novel chemical modifications. *Eur. J. Biochem.*, **270**, 1628–1644.
3. Dorsett,Y. and Tuschl,T. (2004) siRNAs: applications in functional genomics and potential as therapeutics. *Nat. Rev. Drug Discov.*, **3**, 318–329.
4. Nielsen,P.E. and Egholm,M. (1999) Introduction to peptide nucleic acid. *Curr. Issues Mol. Biol.*, **1**, 89–104.
5. Nielsen,P.E. (2006) Addressing the challenges of cellular delivery and bioavailability of peptide nucleic acids (PNA). *Q. Rev. Biophys.*, **38**, 1–6.
6. Koppelhus,U. and Nielsen,P.E. (2003) Cellular delivery of peptide nucleic acid. *Adv. Drug. Deliv. Rev.*, **55**, 267–280.
7. Deshayes,S., Morris,M.C., Divita,G. and Heitz,F. (2005) Cell-penetrating peptides: tools for intracellular delivery of therapeutics. *Cell. Mol. Life Sci.*, **16**, 1839–1849.
8. Järver,P. and Langel,Ü. (2004) The use of cell-penetrating peptides as a toll for gene regulation. *Drug Discov. Today*, **9**, 395–402.
9. Gupta,B., Levchenko,T.S. and Torchilin,V.P. (2005) Intracellular delivery of large molecules and small particles by cell-penetrating proteins and peptides. *Adv. Drug Deliv. Rev.*, **57**, 637–651.
10. Schwarze,S.R., Ho,A., Vocero-Akbani,A. and Dowdy,S.F. (1999) *In vivo* protein transduction: delivery of a biologically active protein into the mouse. *Science*, **285**, 1569–1572.
11. Pooga,M., Soomets,U., Hallbrink,M., Valkna,A., Saar,K., Rezaei,K., Kahl,U., Hao,J.X., Xu,X.J. *et al.* (1998) Cell penetrating PNA constructs regulate galanin receptor levels and modify pain transmission in vivo. *Nat. Biotechnol.*, **16**, 857–861.
12. Bendifallah,N., Rasmussen,F.W., Zachar,V., Ebbesen,P., Nielsen,P.E. and Koppelhus,U. (2006) Evaluation of cell-penetrating peptides (CPPs) as vehicles for intracellular delivery of antisense peptide nucleic acid (PNA). *Bioconjug. Chem.*, **17**, 750–758.
13. Gait,M.J. (2003) Peptide-mediated cellular delivery of antisense oligonucleotides and their analogues. *Cell. Mol. Life Sci.*, **60**, 844–853.
14. Turner,J.J., Ivanova,G.D., Verbeure,B., Williams,D., Arzumanov,A.A., Abes,S., Lebleu,B. and Gait,M.J. (2005) Cell-penetrating peptide conjugates of peptide nucleic acids (PNA) as inhibitors of HIV-1 Tat-dependent trans-activation in cells. *Nucleic Acids Res.*, **33**, 6837–6849.
15. Sazani,P., Vacek,M.M. and Kole,R. (2002) Short-term and long-term modulation of gene expression by antisense therapeutics. *Curr. Opin. Biotechnol.*, **13**, 468–472.
16. Morris,M.C., Vidal,P., Chaloin,L., Heitz,F. and Divita,G. (1997) A new peptide vector for efficient delivery of oligonucleotides into mammalian cells. *Nucleic Acids Res.*, **25**, 2730–2736.
17. Morris,M.C., Depollier,J., Mery,J., Heitz,F. and Divita,G. (2001) A peptide carrier for the delivery of biologically active proteins into mammalian cells. *Nat. Biotechnol.*, **19**, 1173–1176.
18. Simeoni,F., Morris,M.C., Heitz,F. and Divita,G. (2003) Insight into the mechanism of the peptide-based gene delivery system MPG: implications for delivery of siRNA into mammalian cells. *Nucleic Acids Res.*, **31**, 2717–2724.
19. Morris,M.C., Chaloin,L., Choob,M., Archdeacon,J., Heitz,F. and Divita,G. (2004) The combination of a new generation of PNAs with a peptide-based carrier enables efficient targeting of cell cycle progression. *Gene Ther.*, **11**, 757–764.
20. Nan,L., Wu,Y., Bardag-Gorce,F., Li,J., French,B.A., Wilson,L.T., Khanh Nguyen,S. and French,S.W. (2005) RNA interference of VCP/p97 increases Mallory body formation. *Exp. Mol. Pathol.*, **78**, 1–9.

21. Efimov,V., Choob,M., Buryakova,A., Phelan,D. and Chakhmakhcheva,O. (2001) PNA-related oligonucleotide mimics and their evaluation for nucleic acid hybridization studies and analysis. *Nucleosides Nucleotides Nucleic Acids*, **20**, 419–428.
22. Umekita,Y., Hiipakka,R.A., Kokontis,J.M. and Liao,S. (1996) Human prostate tumor growth in athymic mice: inhibition by androgens and stimulation by finasteride. *Proc. Natl Acad. Sci. U.S.A.*, **93**, 11802–11807.
23. Deshayes,S., Heitz,A., Morris,M.C., Charnet,P., Divita,G. and Heitz,F. (2004) Insight into the mechanism of internalization of the cell-penetrating carrier peptide Pep-1 through conformational analysis. *Biochemistry*, **43**, 1449–1457.
24. Pujals,S., Fernandez-Carneado,J., Lopez-Iglesias,C., Kogan,M.J. and Giralt,E. (2006) Mechanistic aspects of CPP-mediated intracellular drug delivery: relevance of CPP self-assembly. *Biochim. Biophys. Acta*, **1758**, 264–279.
25. Wadia,J., Stan,R.V. and Dowdy,S.F. (2004) Transducible TAT-HA fusogenic peptide enhances escape of TAT-fusion proteins after lipid raft macropinocytosis. *Nat. Med.*, **10**, 310–315.
26. Richard,J.P., Melikov,K., Vives,E., Ramos,C., Verbeure,B., Gait,M.J, Chernomordik,L.V. and Lebleu,B. (2003) Cell-penetrating peptides. A reevaluation of the mechanism of cellular uptake. *J. Biol. Chem.*, **278**, 585–590.
27. Morgan,D.O. (1997) Cyclin-dependent kinases: engines, clocks, and microprocessors. *Annu. Rev. Cell Dev. Biol.*, **13**, 261–291.
28. Gleave,M.E. and Monia,B.P. (2005) Antisense therapy for cancer. *Nat. Rev. Cancer*, **5**, 468–479.
29. Yuan,J., Yan,R., Krämer,A., Eckerdt,F., Roller,M., Kaufmann,M. and Strebhardt,K. (2004) Cyclin B1 depletion inhibits proliferation and induces apoptosis in human tumor cells. *Oncogene*, **23**, 5843–5852.
30. Veronese,F.M and Pasut,G. (2005) PEGylation, successful approach to drug delivery. *Drug Discov. Today*, **10**, 1451–1458.
31. Urtishak,K.A, Choob,M., Tian,X., Sternheim,N., Talbot,WS., Wickstrom,E. and Farber,S.A. (2003) Targeted gene knockdown in zebrafish using negatively charged peptide nucleic acid mimics. *Dev. Dyn.*, **228**, 405–413.
32. Efimov,V.A., Birikh,K.R., Staroverov,D.B., Lukyanov,S.A., Tereshina,M.B., Zaraisky,A.G. and Chakhmakhcheva,O.G. (2006) Hydroxyproline-based DNA mimics provide an efficient gene silencing in vitro and in vivo. *Nucleic Acids Res.*, **34**, 2247–2257.